for a boron to bear nearly half a negative (B1 in $B_4H_9^-$, **10**) or half a positive charge (in 1,5-$C_2B_3H_5$, **12**). The plots in Figure 5 illustrate that there is no general relationship between ^{11}B chemical shifts and total atomic charges. While one might perceive a trend for the binary boron hydrides in the plot vs NPA charges (○ and △ in Figure 5b), this is not found at all for the carboranes (□). Boron atoms attached to the more electronegative carbon appear to be more positively charged. However, this is not reflected in the ^{11}B chemical shifts.

The apical borons B1 in the series of pentagonal pyramids **17-20** (the □ in lower half of Figure 5b) are unique in showing exceptionally strong upfield shifts with respect to the computed charges. This might support the ring current models that have been proposed to explain proton NMR chemical shifts of substituted compounds.[73]

Conclusions

The ^{11}B chemical shifts of several boron hydrides and carboranes have been calculated ab initio using the IGLO method. Except for the two smallest carboranes, the agreement between theoretical and experimental values is excellent provided accurate geometries are employed (e.g., optimized ab initio with inclusion of electron correlation). A correct description of δ ^{11}B chemical shifts in carboranes is somewhat more demanding with respect to the level of theory employed: in many cases, the larger TZP type basis II' is needed in order to reproduce the experimental results. The accuracy that can be achieved is remarkable: although two of the observed boron resonances of B_8H_{12} differ by merely 2 ppm, an alternative assignment is suggested by the IGLO calculations.

The effect of counterions on geometry and chemical shifts is shown to be very small in the case of $B_3H_8^-$. Hence, even the treatment of anions as isolated molecules seems justified, and no inherent errors are apparent.

A pessimistic opinion states only two years ago, "...theoretical calculations of these NMR characteristics are of little importance because they cannot be performed as accurately as necessary for the structural elucidation of boron compounds"[38] no longer is valid. A certain limitation, however, is that this accuracy—at least in the case of polyhedral boranes—can only be achieved for geometries optimized at a correlated level (these optimizations can be rather expensive, e.g., 50000 CPU s for the MP2/6-31G* optimization of B_6H_{12} on a CRAY-YMP).

Acknowledgment. This work was supported by the Deutsche Forschungsgemeinschaft, Fonds der Chemischen Industrie, Stiftung Volkswagenwerk, and the Convex Computer Corporation. Computer time was provided by the KFA Jülich. A grant of the Studienstiftung des deutschen Volkes for M.B. is greatfully acknowledged.

Registry No. 1, 19287-45-7; **2**, 18283-29-9; **3**, 19624-22-7; **4**, 18433-84-6; **5**, 23777-80-2; **6**, 12008-19-4; **7a**, 19469-16-0; **8a**, 27380-11-6; **9a**, 12429-74-2; **10**, 12429-85-5; **11**, 90171-84-9; **12**, 20693-66-7; **13**, 26249-71-8; **14**, 55188-36-8; **15**, 20693-67-8; **16**, 20693-68-9; **17**, 12385-35-2; **18**, 18972-20-8; **19**, 12403-04-2; **20**, 28323-17-3; **21**, 20693-69-0.

Supplementary Material Available: Cartesian coordinates of the MP2/6-31G* optimized structures of **1-21** (7 pages). Ordering information is given on any current masthead page.

The Structural Variations of Monomeric Alkaline Earth MX_2 Compounds (M = Ca, Sr, Ba; X = Li, BeH, BH_2, CH_3, NH_2, OH, F). An ab Initio Pseudopotential Study

Martin Kaupp and Paul v. R. Schleyer

Contribution from the Institut für Organische Chemie I, Friedrich-Alexander Universität Erlangen-Nürnberg, Henkestrasse 42, D-8520 Erlangen, Germany. *Received May 10, 1991*

Abstract: The geometries of a series of monomeric alkaline earth MX_2 compounds (M = Ca, Sr, Ba; X = Li, BeH, BH_2, CH_3, NH_2, OH, F) have been calculated at the Hartree-Fock level, using quasirelativistic pseudopotentials for Ca, Sr, and Ba. The energies of fully optimized structures are compared with those of linear X-M-X geometries. Most barium compounds studied (except $BaLi_2$) are bent with angles between 115 and 130° and linearization energies up to ca. 8 kcal/mol (for $Ba(CH_3)_2$). The degree of bending for M = Sr is smaller but is still significant (except for X = Li, BeH). However, most of the Ca compounds may be termed quasilinear, i.e., they either are linear or nearly so and bend easily. The XMX bond angles for M = Sr, Ba do not decrease monotonously along the series X = Li, BeH, BH_2, CH_3, NH_2, OH, F but show a minimum for X = CH_3! Natural atomic orbital population analyses indicate the larger angles with O, N, and F to be due to π-type interactions of lone pairs with empty metal d-orbitals. These $p_\pi \rightarrow d_\pi$ interactions tend to favor linear structures. For the diamides (X = NH_2), significant π-bonding contributions lead to a preference for C_{2v} structures with the hydrogen atoms in the N-M-N plane over C_s or out-of-plane C_{2v} geometries. The barriers to rotation around the M-N bonds are significant. For X = BH_2, C_s and out-of-plane C_{2v} arrangements are slightly more favorable than an in-plane C_{2v} geometry. The dimethyl compounds generally exhibit almost free MCH_3 rotation.

Introduction

Inorganic chemistry textbooks usually treat the chemistry of Ca, Sr, and Ba (e.g., the bioinorganic chemistry of Ca) as that of completely ionic systems, neglecting covalent bonding contributions or even any deviations from a rigid spherical dication model. These assumptions may well be justified in some respects. However, the bent structures of some monomeric dihalides of the heavier group 2 elements are major exceptions to the valence shell electron pair repulsion (VSEPR) model.[1] This is also true for all other common structural models for main group chemistry,[2] including those based only on coulombic forces, assuming completely ionic bonding. There is continuing experimental and

(1) Gillespie, R. J.; Nyholm, R. S. *Quart. Rev.* **1957**, *11*, 339. Gillespie, R. J. *J. Am. Chem. Soc.* **1960**, *82*, 5978. Gillespie, R. S. *J. Chem. Educ.* **1970**, *47*, 18. Gillespie, R. J.; Hargittai, I. *The VSEPR Model of Molecular Geometry*; Allyn and Bacon: Boston, MA, 1991.

(2) Cotton, F. A.; Wilkinson, G. *Advanced Inorganic Chemistry*, 5th ed.; Wiley: New York, 1988.

0002-7863/92/1514-491$03.00/0

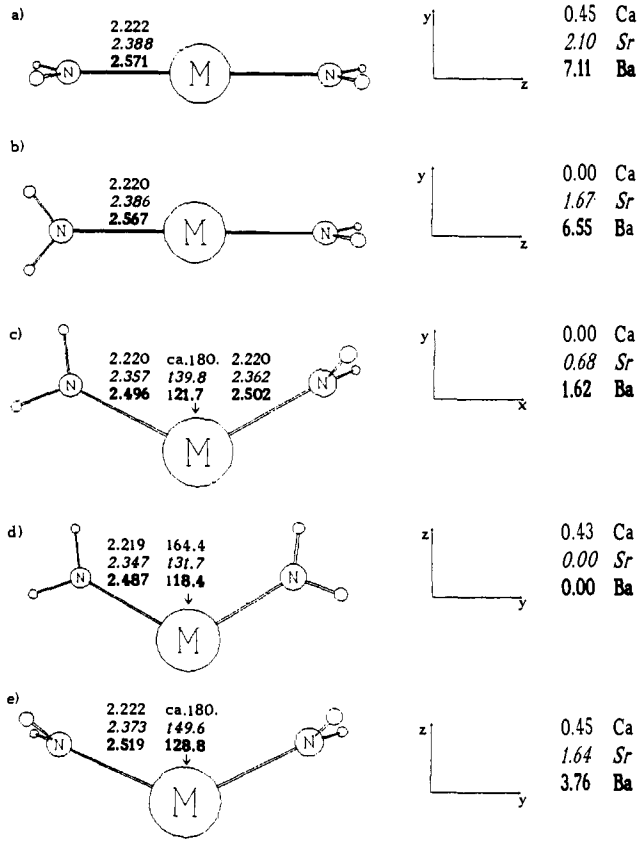

Figure 1. Optimized structures for $M(NH_2)_2$ (in the order M = Ca, *Sr*, **Ba**) illustrated by plots for $Ba(NH_2)_2$. The axes demonstrate the orientation conventions for these symmetries, important for orbital designations. Distances are given in Å, angles in deg. The energies relative to the most stable structure are given on the right side in kcal/mol. The N–H distances generally are ca. 1.003–1.005 Å, the H–N–H angles are ca. 102.8-104.6°: (a) D_{2h}, (b) D_{2d}, (c) C_s, (d) C_{2v}^{ip}, and (e) C_{2v}^{op}.

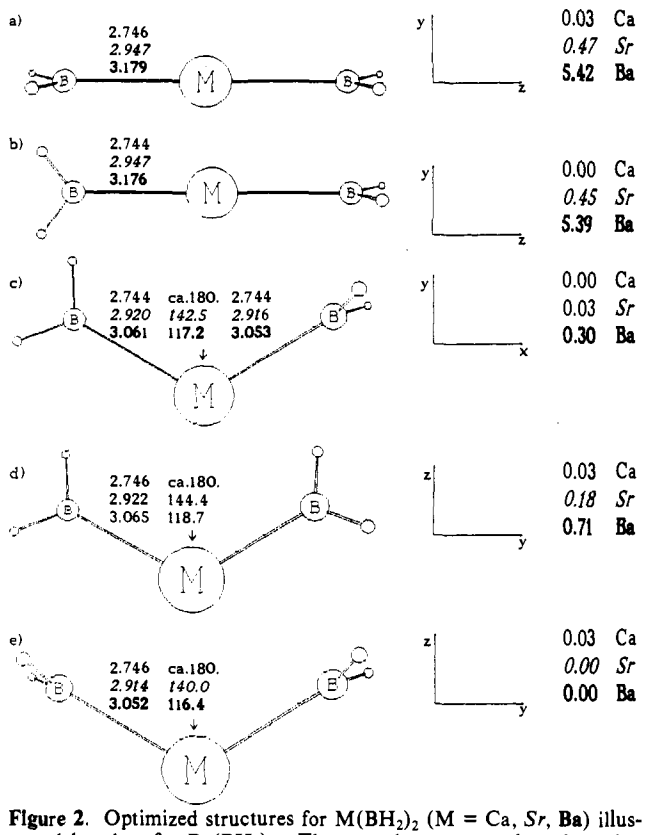

Figure 2. Optimized structures for $M(BH_2)_2$ (M = Ca, *Sr*, **Ba**) illustrated by plots for $Ba(BH_2)_2$. The axes demonstrate the orientation conventions for these symmetries, important for orbital designations. Distances are given in Å, angles in deg. The energies relative to the most stable structure are given on the right side in kcal/mol. The B–H distances are ca. 1.204, *1.206*, **1.210** Å for M = Ca, *Sr*, **Ba**, respectively; the H–B–H angles generally are between 108.5 and 110.4°: (a) D_{2h}, (b) D_{2d}, (c) C_s, (d) C_{2v}^{ip}, and (e) C_{2v}^{op}.

theoretical activity to establish the structures of these molecules. The difficulties associated with experimental structure determinations of these species have been reviewed.[3-5] Two recent independent computational studies of the complete set of alkaline earth dihalides[3,4] have confirmed that several of these species are significantly bent, whereas others either are genuinely linear or exhibit extremely shallow bending potentials and should be termed "quasilinear".[4] Several species (e.g., BaF_2, SrF_2, $BaCl_2$) are distinctly bent; this allowed the computational evaluation of relatively accurate angles[3,4] and of the energies necessary for linearization.[3]

Small covalent contributions to the bonding, interionic repulsions, and the polarization of the cations and the anions influence the bent or linear structural preferences.[3,6] From an orbital-oriented viewpoint, both d-orbital participation in the small metal valence populations and the polarization of the subvalence shell contribute to the bending.[3,6] This reconciles the "d-hybridization" and "polarized-ion" models that were once discussed controversially.[2]

Reinforced by recent gas-phase electron diffraction results on the substituted metallocenes MCp_2^* ($Cp^* = \eta_5$-C_5Me_5, M = Ca, Sr, Ba)[7] and by our computational investigation of the Ca, Sr, and Ba dihydrides,[6] the bending tendencies observed for the dihalides may be expected to be general for derivatives of the heavier group 2 elements. In view of the excellent performance of the 10 valence electron pseudopotential approach for the Ca, Sr, and Ba dihalides[3] and dihydrides[6] it seems worthwhile to extend our previous results for MF_2[3] to the entire set of structures for the basic first-row substituents (X = Li, BeH, BH_2, CH_3, NH_2, OH, F). Are the changes in bending for the different substituents systematic? Do they correlate with other characteristics of these groups? Except for the dihalides,[3,4,5,8] dihydrides,[6,8f,h] and the metallocenes,[7] neither experimental nor previous computational data are available for monomeric MX_2 compounds of Ca, Sr, and Ba.

Computational Details

The same quasirelativistic 10 valence electron pseudopotentials and the corresponding 6s6p5d valence basis sets for Ca, Sr, and Ba we described elsewhere[6] were used. For the first-row elements, pseudopoten-

(3) Kaupp, M.; Schleyer, P. v. R.; Stoll, H.; Preuss, H. *J. Am. Chem. Soc.* **1991**, *113*, 6012.

(4) Seijo, L.; Barandiaran, Z.; Huzinaga, S. *J. Chem. Phys.* **1991**, *94*, 3762.

(5) For recent reviews on the determination of metal halide gas-phase structures, see: Hargittai, M. *Coord. Chem. Rev.* **1988**, *91*, 35. Hargittai, M. In *Stereochemical Applications of Gas Phase Electron Diffraction*; Hargittai, I., Hargittai, M., Eds.; Verlag Chemie: Weinheim, 1988; Part B, pp 383–454.

(6) Kaupp, M.; Schleyer, P. v. R.; Stoll, H.; Preuss, H. *J. Chem. Phys.* **1991**, *94*, 1360.

(7) (a) Andersen, R. A.; Boncella, J. M.; Burns, C. J.; Blom, R.; Haaland, A.; Volden, H. V. *J. Organomet. Chem.* **1986**, *312*, C49. Andersen, R. A.; Blom, R.; Boncella, J. M.; Burns, C. J.; Volden, H. V. *Acta Chem. Scand.* **1987**, *A41*, 24. Andersen, R. A.; Blom, R.; Burns, J. M.; Volden, H. V. *J. Chem. Soc., Chem. Commun.* **1987**, 768. Blom, R.; Faegri, K., Jr.; Volden, H. V. *Organometallics* **1990**, *9*, 372. (b) We have found evidence for linear equilibrium structures of calcocene and strontocene and a quasilinear behavior of barocene: Kaupp, M.; Schleyer, P. v. R.; Dolg, M.; Stoll, H., submitted to *J. Am. Chem. Soc.*

(8) (a) Gole, J. L.; Siu, A. K. Q.; Hayes, E. F. *J. Chem. Phys.* **1973**, *58*, 857. (b) Yarkony, D. R.; Hunt, W. J.; Schaefer III, H. F. *Mol. Phys.* **1973**, *26*, 941. (c) Klimenko, N. M.; Musaev, D. G.; Charkin, O. P. *Russ. J. Inorg. Chem.* **1984**, *29*, 639. (d) v. Szentpály, L.; Schwerdtfeger, P. *Chem. Phys. Lett.*, **1990**, *170*, 555. (e) Salzner, U.; Schleyer, P. v. R. *Chem. Phys. Lett.*, **1990**, *172*, 461. (f) Hassett, D. M.; Marsden, C. J. *J. Chem. Soc., Chem. Commun.* **1990**, 667. (g) Dyke, J. M.; Wright, T. G. *Chem. Phys. Lett.* **1990**, *169*, 138. (h) DeKock, R. L.; Peterson, M. A.; Timmer, L. K.; Baerends, E. J.; Vernooijs, P. *Polyhedron* **1990**, *9*, 1919.

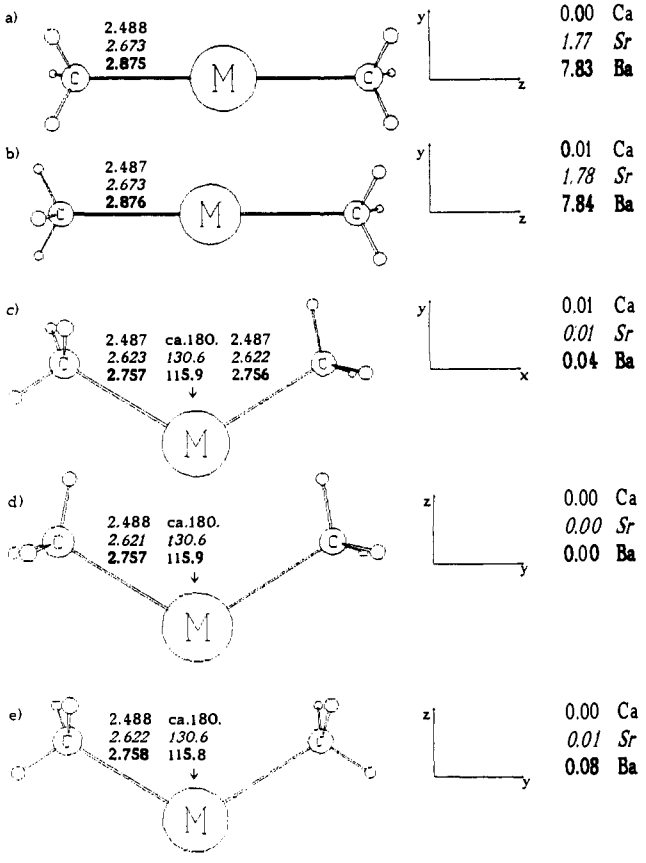

Figure 3. Optimized structures for $M(CH_3)_2$ (M = Ca, *Sr*, **Ba**) illustrated by plots for $Ba(CH_3)_2$. The axes demonstrate the orientation conventions for these symmetries, important for orbital designations. Distances are given in Å, angles in deg. The energies relative to the most stable structure are given on the right side in kcal/mol. The C–H distances generally are ca. 1.093–1.096 Å; the H–C–M angles are ca. 110.9–114.6°: (a) D_{3h}, (b) D_{3d}, (c) C_s, (d) C_{2v}^2, and (e) C_{2v}^4.

tials replace the He core.[9,10a] For Li and Be two p-functions and one d-polarization function[11a] have been added to the [4s]/(3s) valence basis sets[11b] to give [4s2p1d]/(3s2p1d) sets. The valence bases for B, C, N, and O consist of [4s4p]/(2s2p) sets,[11b] augmented by diffuse sp[11c] and d-polarization functions,[11a] to yield [5s5p1d]/(3s3p1d) valence basis sets similar to those used (with quasirelativistic pseudopotentials[10]) for the dihalides.[3] For hydrogen, the [4s1p]/(2s1p) basis set of Dunning and Hay[12] has been employed.

All geometries have been fully optimized although symmetry restrictions have been imposed for special cases. The conformations considered for $M(NH_2)_2$, $M(BH_2)_2$, $M(CH_3)_2$, and $M(OH)_2$ are shown in Figures 1–4. For X = BH_2 or NH_2, two linear structures are conceivable (D_{2h} and D_{2d}), corresponding to eclipsed or staggered arrangements of the two substituent groups (Figures 1a,b and 2a,b). Three bent geometries have been examined: C_s with staggered substituents (Figures 1c and 2c), C_{2v} with all hydrogen atoms in the XMX plane (C_{2v}^{ip}; Figures 1d and 2d), and C_{2v} with all hydrogens out-of-plane (C_{2v}^{op}; Figures 1e and 2e). For linear $M(CH_3)_2$, eclipsed D_{3h} and staggered D_{3d} geometries have been compared (Figure 3a,b). For bent arrangements, the staggered C_s geometry (Figure 3c) and two eclipsed C_{2v} structures (with either two or four hydrogen atoms approaching each other upon bending; Figure 3d,e) were examined

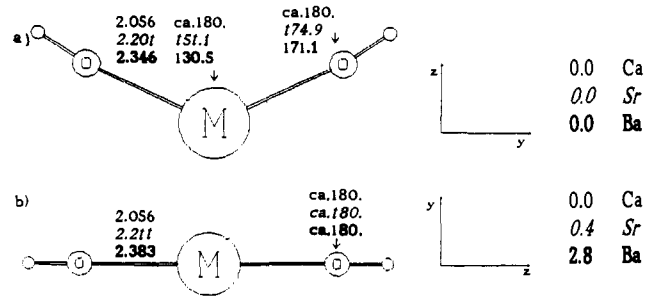

Figure 4. Optimized geometries for $M(OH)_2$ (M = Ca, *Sr*, **Ba**) illustrated by plots for $Ba(OH)_2$. The axes demonstrate the orientation conventions for these symmetries, important for orbital designations. Distances are given in Å, angles in deg. The energies relative to the most stable structure are given on the right side in kcal/mol. The O–H distances are 0.935, *0.936*, **0.937** Å for M = Ca, *Sr*, **Ba**, respectively: (a) C_2 and (b) C_{2h} ($\rightarrow D_{\infty h}$).

Table I. Metal–Ligand Distances R(MX) (Å) and Bond Lengthening upon Linearization ΔR_1 (Å) for Alkaline Earth MX_2 Compounds

	Ca		Sr		Ba	
X	R(MX)	ΔR_1	R(MX)	ΔR_1	R(MX)	ΔR_1
Li	3.369		3.565		3.807	
BeH	3.022		3.235		3.413	0.070
BH_2[a]	2.746		2.914	0.033	3.052	0.126
CH_3	2.487		2.621	0.052	2.757	0.180
NH_2[b]	2.219	0.001	2.347	0.039	2.487	0.080
OH	2.056		2.201	0.010	2.346	0.037
F	2.029	0.004	2.164	0.022	2.299	0.053

[a] The values pertaining to C_{2v}^{op} (bent) and D_{2h} (linear) structures are given (cf. Figure 2). [b] The values pertaining to C_{2v}^{ip} (bent) and D_{2d} (linear) structures are given (cf. Figure 1).

for each metal. For X = BeH or OH, we optimized geometries in C_2 (bending angle <180°) and in C_{2h} symmetries (XMX = 180°). However, the optimization converged toward geometries close to the corresponding C_{2v} and $D_{\infty h}$ structures with near-linear coordination around O or Be (cf. Figure 4). C_{2v} and $D_{\infty h}$ structures also are compared for MF_2[3] and for MLi_2.

All geometry optimizations and frequency calculations at the Hartree–Fock level of theory were carried out with the GAUSSIAN 88 program,[13] employing standard gradient optimization techniques. Additional quadratic configuration interaction optimizations including single, double, and (perturbationally) triple substitutions (QCISD(T))[14] for MLi_2 have been performed via a quadratic fit to single point calculations. Natural population analyses employed Reed's GAUSSIAN 88 adaptation of the NBO program.[15]

Results and Discussion

A. Geometries. Table I summarizes the calculated MX distances for the fully optimized structures (in the most stable conformations) and also the increases in bond lengths observed in going from bent to linear geometries. Table II gives the bending angles and the linearization energies. See Figures 1–4 for more details.

Consistent with the substituent electronegativities[16] and also with the ionic or covalent radii for the first-row elements,[17] the MX distances decrease monotonously when going down a R(MX)

(9) (a) Fuentealba, P.; v. Szentpály, L.; Preuss, H.; Stoll, H. *J. Phys. B* **1985**, *73*, 1287. (b) Igel-Mann, G.; Stoll, H.; Preuss, H. *Mol. Phys.* **1988**, *65*, 1321.

(10) (a) Dolg, M. Ph.D. Thesis, University of Stuttgart, 1989. (b) Schwerdtfeger, P.; Dolg, M.; Schwarz, W. H. E.; Bowmaker, G. A.; Boyd, P. D. W. *J. Chem. Phys.* **1989**, *91*, 1762.

(11) (a) *Gaussian Basis Sets for Molecular Calculations*; Huzinaga, S., Ed.; Elsevier: New York, 1984. (b) Poppe, J.; Igel-Mann, G.; Savin, A.; Stoll, H., unpublished results. Kaupp, M.; Stoll, H.; Preuss, H. *J. Comput. Chem.* **1990**, *11*, 1029. (c) Clark, T.; Chandrasekhar, J.; Spitznagel, G. W.; Schleyer, P. v. R. *J. Comput. Chem.* **1983**, *4*, 294.

(12) Dunning, T. H.; Hay, H. In *Methods of Electronic Structure Theory*; (Modern Theoretical Chemistry, Vol. 3), Schaefer III, H. F., Ed.; Plenum Press: 1977; p 1ff.

(13) Frisch, M. J.; Head-Gordon, M.; Schlegel, H. B.; Raghavachari, K.; Binkley, J. S.; Gonzalez, C.; DeFrees, D. J.; Fox, D. J.; Whiteside, R. A.; Seeger, R.; Melius, C. F.; Baker, J.; Kahn, L. R.; Stewart, J. J. P.; Fluder, E. M.; Topiol, S.; Pople, J. A. Gaussian, Inc.: Pittsburgh, PA.

(14) Pople, J. A.; Head-Gordon, M.; Raghavachari, K. *J. Chem. Phys.* **1987**, *87*, 5968.

(15) Reed, A. E.; Weinstock, R. B.; Weinhold, F. *J. Chem. Phys.* **1985**, *83*, 735. Reed, A. E.; Weinhold, F. *J. Chem. Phys.* **1985**, *83*, 1736. Reed, A. E.; Curtiss, L. A.; Weinhold, F. *Chem. Rev.* **1988**, *88*, 899.

(16) Mullay, J. *J. Am. Chem. Soc.* **1984**, *106*, 5842. Marriott, S.; Reynolds, W. F.; Taft, R. W.; Topsom, R. D. *J. Org. Chem.* **1984**, *49*, 959. Boyd, R. J.; Edgecombe, K. E. *J. Am. Chem. Soc.* **1988**, *110*, 4182. Pearson, R. G. *Inorg. Chem.* **1988**, *27*, 734.

(17) See, e.g.: *Lange's Handbook of Chemistry*, 13th ed.; Dean, J. A., Ed.; McGraw Hill: 1985.

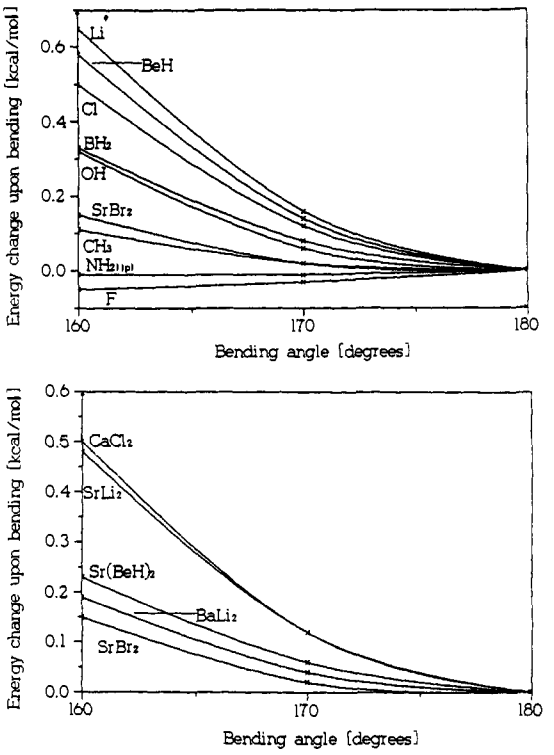

Figure 5. (a) Energy change with bending angle for various CaX_2 compounds and $SrBr_2$. (b) Energy change with bending angle for some MX_2 compounds of Ca, Sr, and Ba.

column of Table I. As the Hartree–Fock calculations do not consider the bond-contracting effect of core valence correlation (known to be considerable for these metals),[3,6,18] the MX distances in Table I probably are all overestimated. The bond length contraction due to these inter-shell correlation effects depends both on the strength of the bond and on the availability of low-lying virtual orbitals. The magnitude of the contraction may be expected to decrease strongly from X = Li to X = F. Optimization of the M–Li distances at the QCISD(T) level of theory[14] (one f-function added to the metal basis sets[6]) reduces the distances given in Table I by 13.5, 15.3, and 18.5 pm to 3.234, 3.412, and 3.622 Å for $CaLi_2$, $SrLi_2$, and $BaLi_2$, respectively. The corresponding contractions at the size consistency corrected CISD level for the difluoride M–F distances have been found to be only 1.9, 0.3, and 4.5 pm for CaF_2, SrF_2 and BaF_2, respectively.[3] The difluoride bond lengths (in contrast to those for the other Ca, Sr, and Ba dihalides) are shorter than the reported experimental values, but we strongly doubt the accuracy of these experimental data.[3] Thus, interpolation between the differences in the bond distances at the HF and correlated levels for MLi_2 and MF_2 (for a given M) and subtraction of the obtained value from the Hartree–Fock results should allow satisfactory estimates for the M–X distances in the other species.

As expected,[3,4,6] the degree of bending for a given substituent increases with the heavier metals. All the Ca compounds studied are linear or nearly so. While $Ca(NH_2)_2$ shows some deviation from linearity for the C_{2v}^{op} structure, only CaF_2 is bent at the level of theory used. The angle (152.3°) and linearization energy (0.06 kcal/mol) confirm the very shallow bending potential that has made the theoretical study of CaF_2 such a demanding task.[3,4,8] The quite shallow bending potentials of the other Ca compounds are shown by our calculations at various bending angles (but keeping all other parameters fixed at the optimized values, see Table III and Figure 5a). $CaLi_2$ and $Ca(BeH)_2$ are indicated

(18) Pettersson, L. G. M.; Siegbahn, P. E. M.; Ismail, S. *Chem. Phys.* **1983**, *82*, 355. Partridge, H.; Bauschlicher, C. W.; Walch, S. P.; Liu, B. *J. Chem. Phys.* **1983**, *72*, 1866. Fuentealba, P.; Reyes, O.; Stoll, H.; Preuss, H. *J. Chem. Phys.* **1987**, *87*, 5338. Jeung, G.; Daudey, J.-P.; Malrieu, J.-P. *Chem. Phys. Lett.* **1983**, *98*, 433.

Table II. Bending Angles XMX [deg] and Linearization Energies ΔE_1 (kcal/mol) for SrX_2 and BaX_2 Compounds

	Sr		Ba	
X	XMX	ΔE_1	XMX	ΔE_1
Li	linear		linear	
BeH	linear		128.8	1.55
BH_2[a]	140.0	0.47	116.4	5.42
CH_3	130.6	1.77	115.9	7.83
NH_2[b]	131.7	1.67	118.4	6.55
OH	151.1	0.42	130.5	2.79
F	141.5	1.23	125.6	4.30

[a] The values pertaining to C_{2v}^{op} (bent) and D_{2h} (linear) structures are given (cf. Figure 2). [b] The values pertaining to C_{2v}^{ip} (bent) and D_{2d} (linear) structures are given (cf. Figure 1).

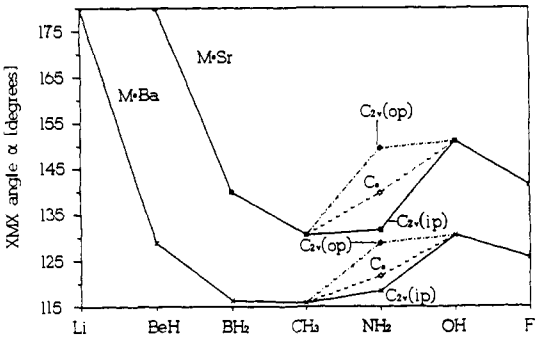

Figure 6. XMX angles for SrX_2 and BaX_2 compounds (X = Li, BeH, BH_2, CH_3, NH_2, OH, F). For X = NH_2, points for structures with all hydrogen atoms in the NMN plane (C_{2v}^{ip}), all hydrogens out-of-plane (C_{2v}^{op}), and two hydrogens out-of-plane (C_s) are included (cf. Figure 1).

to be linear with slightly deeper potential wells than that for the reputedly linear[3-5,8e,h,i] $CaCl_2$. The bending potentials for $Ca(BH_2)_2$ and $Ca(OH)_2$ are intermediate between those for $CaCl_2$ and $SrBr_2$. Strontium dibromide, described as quasilinear by Seijo et al.,[4] is borderline between linear and bent.[3] There is almost no variation in energy when the angle is decreased by ca. 20–30° from linearity. The bending potentials for monomeric dimethylcalcium and calcium diamide (in the C_{2v}^{ip} conformation) are even more shallow than that for $SrBr_2$. These molecules (and CaF_2) definitely are quasilinear. The same is true for $BaLi_2$ and $Sr(BeH)_2$, but the linear preference for $SrLi_2$ is greater (cf. Table III and Figure 5b). The harmonic frequencies and force constants for the MLi_2 species (see Table IV) support these conclusions further. Accurate prediction of the angles is very difficult for compounds with extremely shallow bending potentials. The structure of some of the quasilinear species may change from linear to bent or vice versa when more accurate calculations, involving larger basis sets and electron correlation corrections, are carried out. However, the exact molecular equilibrium structures are not very meaningful for such molecules.

In this respect, the data for most of the strontium and particularly for the barium compounds are more conclusive than for the CaX_2 species (see Tables I and II). Obviously, several of these Sr and Ba molecules are bent quite significantly. In particular, the monomeric dimethyl compounds have small XMX angles which are even lower than those of the difluorides.[3,4] As correlation corrections generally influence the degree of dihalide and dihydride bending only moderately (at least in cases where the bending potential is not exceedingly flat),[3,6,8e-h] many of the predicted angles in Table I and of the linearization energies in Table II should be reasonably accurate (particularly for M = Ba).

B. π-Effects. There are no monotonous trends in the bending angles or linearization energies in going from X = Li to X = F, i.e., down the columns in Tables I and II (cf. Figures 6–8 for graphical representations). The XMX angles for the Sr and Ba compounds decrease in going from X = Li to X = CH_3, increase for X = NH_2 and OH, and then decrease again with X = F. A similar trend (the position of X = NH_2 is slightly different) is observed for the bending potentials of the Ca compounds, but note that the energy differences involved are very small (cf. Table III,

Table III. Energy Change (kcal/mol) upon Bending for Various Linear or Quasilinear MX_2 Compounds of Ca, Sr, and Ba

bending angle[a]	$CaLi_2$	$Ca(BeH)_2$	$Ca(BH_2)_2$	$Ca(CH_3)_2$	$Ca(NH_2)_2$[b]	$Ca(OH)_2$
180	0.00	0.00	0.00	0.00	0.00	0.00
170	0.16	0.14	0.08	0.02	−0.01	0.06
160	0.65	0.58	0.33	0.11	−0.01	0.32
bending angle[a]	CaF_2	$CaCl_2$	$SrBr_2$	$SrLi_2$	$Sr(BeH)_2$	$BaLi_2$
180	0.00	0.00	0.00	0.00	0.00	0.00
170	−0.03	0.12	0.02	0.12	0.06	0.04
160	−0.05	0.50	0.15	0.48	0.23	0.19

[a] Angles in deg. [b] Energy values for the C_{2v}^{ip} structure (cf. Figure 1) are given.

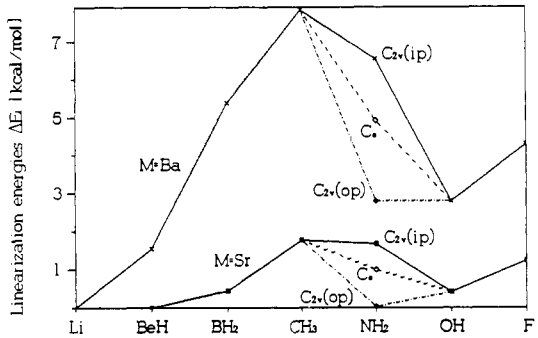

Figure 7. Linearization energies for SrX_2 and BaX_2 compounds (X = Li, BeH, BH_2, CH_3, NH_2, OH, F). For X = NH_2, points for structures with all hydrogen atoms in the NMN plane (C_{2v}^{ip}), all hydrogens out-of-plane (C_{2v}^{op}), and two hydrogens out-of-plane (C_s) are included (cf. Figure 1).

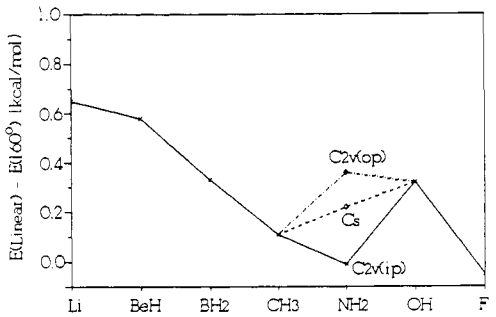

Figure 8. Energy difference between linear and 160° bent structures of CaX_2 compounds. Note the different presentation (energy scale!) from Figures 6 and 7.

Figure 8). The most obvious difference between the X = Li, BeH, BH_2, CH_3 and the X = NH_2, OH, F sets of substituents is the presence of extra lone pairs for the latter group.

(a) The Diamides. The lone pair influences are particularly obvious for X = NH_2, where several characteristic conformations are feasable (cf. Figure 1). As indicated by the sets of points in Figures 6 and 7, and by the energies given in Figure 1, the C_{2v}^{ip} structures, i.e., bent geometries with all NH_2 hydrogen atoms in the NMN planes (cf. Figure 1d), are the most stable conformations for the Sr and Ba diamides. These conformations also exhibit the smallest XMX angles (cf. Figure 1). In particular, $Ba(NH_2)_2$ (note the small NBaN angle) exhibits a sizeable barrier to out-of-plane rotation of one NH_2 group ($\rightarrow C_s$) and even a slightly larger one for the second NH_2 ($\rightarrow C_{2v}^{op}$). The rotated conformations prefer wider XMX angles (up to ca. 10° and 18° for $Ba(NH_2)_2$ and $Sr(NH_2)_2$, respectively). However, if < XMX = 180° is imposed, the staggered D_{2d} structures are slightly more stable than the eclipsed D_{2h} linear forms. Hence, bending results in strong conformational preferences for the NH_2 groups. As the XMX angle is smallest for M = Ba, its rotational barrier is largest; for M = Ca the barrier is negligible (cf. Figure 1).

Obviously the π-lone pairs influence the structures of the diamides significantly. The amide N local geometries are almost planar, even in cases where pyramidalization would not be prohibited by symmetry (C_{2v}^{op}, C_s). This behavior is expected to be due to the highly electropositive metals (see ref 19 for a detailed discussion of substituent π-effects vs electronegativity). Are there covalent bonding contributions to the diamides? How do π-interactions influence the geometries? Natural atomic orbital (NAO) populations of key metal orbitals for the various $Ba(NH_2)_2$ conformations are given in Table V. We concentrate on the barium compound since the effects are largest. (For the other metals, the populations for the linear structures are very similar, with slightly increased s- and p-populations. However, due to the larger angles, the changes in the bent structures are less dramatic. This also holds true for the dihydroxides, difluorides, etc., see below.)

Table IV. Harmonic Vibrational Frequencies ω (cm^{-1}) and Force Constants k (mDyne/Å) for MLi_2(M = Ca, Sr, Ba)

	$\omega(\delta s)$	$\omega(\nu s)$	$\omega(\nu as)$	$k(\delta s)$	$k(\nu s)$	$k(\nu as)$
$CaLi_2$	65	238	266	0.022	0.233	0.372
$SrLi_2$	49	222	230	0.011	0.204	0.251
$BaLi_2$	27	207	209	0.003	0.177	0.197

Table V. Natural Atomic Orbital (NAO) Occupancies for the Ba 5d- and 6s-Orbitals for Different Conformations of $Ba(NH_2)_2$[a]

	molecular symmetry[b]				
NAO	C_{2v}^{ip}	C_s	C_{2v}^{op}	D_{2d}	D_{2h}
6s	0.016	0.015	0.013	0.006	0.006
$5d_{xy}$	0.035	0.046	0.000	0.000	0.000
$5d_{xz}$	0.016	0.020	0.000	0.024	0.042
$5d_{yz}$	0.045	0.008	0.050	0.024	0.000
$5d_{x^2-y^2}$	0.017	0.019	0.021	0.000	0.000
$5d_{z^2}$	0.001	0.014	0.021	0.021	0.022
$5d_{tot.}$	0.114	0.107	0.092	0.069	0.064

[a] The valence p-populations are negligible. [b] Note, that the assignment of coordinate axes is different for C_{2v}, C_s, D_{2d}, and D_{2h} symmetries (see Figure 1).

In the linear (D_{2d} versus D_{2h}) $Ba(NH_2)_2$ systems, the d_π-populations exceed the σ-contributions. The D_{2d} form is favored slightly as two different d_π-NAOs (d_{xz},d_{yz}) can function as acceptor orbitals for the two perpendicular π-lone pairs on the two N atoms. While only one d_π-AO on Ba can be involved in the D_{2h} conformation, the rotational barrier is very small (ca. 0.5 kcal/mol). The d_π-populations for the linear structures are reduced upon bending (note, that by convention for D_{2d} and D_{2h} symmetry the z-axis goes through both nitrogens and the metal, whereas for C_{2v} and C_s symmetries the NMN angles are in the yz- or xy-planes, respectively; see Figure 1). The s- and the net d-populations in Table V document the degree of ligand-to-metal charge transfer which occurs upon bending. This has been noted earlier for the alkaline earth dihalides.[3,8e] For the C_{2v} forms, the major contributions pertain to the d_{yz}-orbital which has σ-symmetry with respect to the two individual M–N bonds. This type of interaction is a major contributor to the bending of the dihalides[3,4,8e-h] and of the dihydrides[6] (in addition to core polarization, which also favors a bent geometry[3,6]). However, the major difference between the C_{2v}^{ip} and C_{2v}^{op} structures involves π-type contributions: in particular, the participation of the d_{xy} and d_{xz}-NAOs for C_{2v}^{ip}. These appear to determine the preference for the C_{2v}^{ip} structure over both the C_{2v}^{op} and the C_s geometries. Thus, small $p_\pi \rightarrow d_\pi$ charge-transfer interactions between nitrogen lone pairs as donors and the appropriate metal d-orbitals as acceptors are responsible for the observed rotational barriers. The importance of these

Table VI. Natural Atomic Orbital (NAO) Occupancies for the Ba 5d- and 6s-Orbitals in $Ba(OH)_2$ and BaF_2[a]

NAO	$Ba(OH)_2$		BaF_2	
	C_{2v}[b]	$D_{\infty h}$[c]	C_{2v}[b]	$D_{\infty h}$[c]
6s	0.006	0.004	0.002	0.004
$5d_{yz}$	0.030	0.019	0.044	0.015
$5d_{xz}$	0.006	0.019	0.005	0.015
$5d_{xy}$	0.017	0.000	0.013	0.000
$5d_{x^2-y^2}$	0.009	0.000	0.023	0.000
$5d_{z^2}$	0.010	0.010	0.009	0.030
$5d_{tot.}$	0.072	0.048	0.094	0.060

[a] The valence p-populations are negligible. [b] Note, that the molecule lies in the *yz*-plane. [c] Note, that the *z*-axis is the molecular axis.

interactions for the barrier decreases when the XMX angles are larger. Therefore, the M–NH_2 rotational barriers are smaller in $Sr(NH_2)_2$ and are negligible in $Ca(NH_2)_2$.

Some experimental results suggest that these π-effects may also be present in oligomeric species: The NSi_2 moieties of the terminal $N(SiMe_3)_2$ groups in dimeric $\{M[N(SiMe_3)_2]_2\}_2$ (M = Sr,[20] Ba[21]) as well as in $NaM[N(SiMe_3)_2]_3$ (M = Eu(II), Yb(II)),[22] lie approximately in the plane defined by the two bridging nitrogens and M. The terminal amide groups in $\{Ca[N(SiMe_3)_2]_2\}_2$, on the other hand, are twisted out-of-plane.[23] Whether these conformational preferences are related to $p_\pi \rightarrow d_\pi$ bonding contributions is not clear, as the π-donor ability of the $N(SiMe_3)_2$ groups may be significantly smaller than that of NH_2 substituents. Preliminary computational results for terminal NH_2 groups in model dimers $[M(NH_2)_2]_2$ and $[HMNH_2]_2$ indicate rotational barriers on the order of ca. 1.5 kcal/mol per amide group (even for M = Ca).[24] The importance of $p_\pi \rightarrow d_\pi$ bonding contributions is well-established for early transition-metal amides.[25,26]

(b) The Dihydroxides and Difluorides. How important are π-effects with OH or F substituents? As the $M(OH)_2$ geometry optimizations converged toward approximately linear M–O–H arrangements, OH^- can be considered to have one σ- and two p_π-lone pairs. In linear geometries these lead to significant π-interactions with metal d_{xz} and d_{yz} NAOs (see Table VI). One of the π-contributions is reduced significantly upon OMO bending. This explains why the XMX angles are significantly larger than for the C_{2v}^{ip} structures of the diamides. But note that the effects for the dihydroxides are of similar magnitude as for the diamide C_{2v}^{op} structures (see Figures 1, 4, and 6–8). Then why does the linearization energy increase (and the angle decrease) in going from X = OH to X = F? Table VI indicates that the π-contributions (d_{xz} and d_{yz}) for linear $Ba(OH)_2$ and BaF_2 are very similar. However, the σ-donor ability of OH^- is reduced, compared to F^- (cf. the metal $5d_{z^2}$ populations for $D_{\infty h}$). Further analysis of the corresponding natural bond orbitals (NBO) reveals a higher percentage of s-character in the σ-donor NBO for OH^- than for F^-. This reduced σ-donor ability (due to the presence of a covalent OH bond in trans position) also is observed for the bent structure (compare the $5d_{yz}$ and $5d_{x^2-y^2}$ populations of bent $Ba(OH)_2$ and BaF_2 in Table VI). Indeed, the dihydroxides seem to be the most ionic of all systems studied (cf. Table VII for the natural population analysis (NPA) net charges). As the σ-bonding contributions favor and the π-type contributions oppose bending, the dihydroxides have larger XMX angles than the difluorides.

(c) $M(BH_2)_2$ and $M(CH_3)_2$. For X = BH_2 and CH_3, π-lone pairs are absent, and the B–H and C–H bonds are not very effective as hyperconjugative π-donors. As expected, only small rotational barriers are observed for these groups. The out-of-plane (C_{2v}^{op}) structure of $Ba(BH_2)_2$ is ca. 0.3 and 0.7 kcal/mol more stable than the C_s and C_{2v}^{ip} structures, respectively (cf. Figure 2). The BBaB angles for these structures differ by less than 3°. Very small effects also are observed for the corresponding conformations of $Sr(BH_2)_2$. The energy difference between the D_{2d} and D_{2h} geometries is negligible (<0.05 kcal/mol). All of the dimethyl compounds (cf. Figure 3) exhibit almost free M–CH_3 rotation (ΔE_R < 0.1 kcal/mol), even for the bent geometries. This indicates that steric effects also are small.

Table VII. NPA Central Metal Net Charges Q and Relative Valence s-, p-, and d-Populations (%) for Alkaline Earth MX_2 Compounds[a]

	linear				bent			
	Q	s	p	d	Q	s	p	d
				M = Ca[a]				
Li	0.526	88.1	10.4	1.5				
BeH	0.762	76.7	18.7	4.6				
BH_2	1.493	91.1	2.0	6.9				
CH_3	1.775	80.3	3.4	16.3				
NH_2	1.906	26.4	8.2	65.4				
OH	1.946	7.0	0.0	93.0				
F	1.924	7.1	5.0	87.9				
				M = Sr				
Li	0.642	88.4	9.5	2.1				
BeH	0.881	75.3	17.4	7.3				
BH_2[b]	1.569	89.5	2.6	7.9	1.529	88.5	0.0	11.5
CH_3	1.822	76.4	4.8	18.8	1.779	73.6	0.0	26.4
NH_2[c]	1.927	17.8	2.3	79.9	1.905	20.7	0.0	79.3
OH	1.960	1.5	0.0	98.5	1.954	3.8	0.0	96.2
F	1.938	4.0	1.6	94.4	1.927	3.7	0.0	96.3
				M = Ba				
Li	0.825	86.0	9.2	4.8				
BeH	1.070	69.2	17.3	13.5	0.973	68.6	10.4	21.0
BH_2[b]	1.691	80.1	4.1	15.8	1.570	72.8	0.9	26.3
CH_3	1.886	55.2	6.6	38.2	1.799	47.3	0.0	52.7
NH_2[c]	1.933	2.4	0.0	97.6	1.895	8.9	0.0	91.1
OH	1.966	0.0	0.0	100.0	1.949	0.1	0.0	99.9
F	1.940	0.7	0.0	99.3	1.921	2.9	0.0	97.1

[a] Percentages of the absolute valence populations (2-Q) are given. As the changes upon bending for CaF_2 and $Ca(NH_2)_2$ are negligible, only the values for linear CaX_2 structures are included. [b] Results for C_{2v}^{op} and D_{2h} structures. [c] Results for C_{2v}^{ip} and D_{2d} structures.

C. The Bonding in MLi_2 and $M(BeH)_2$. The NPA metal net charges given in Table VII show that the bonding in MLi_2 and $M(BeH)_2$ is considerably less ionic than that in the other species studied in this work. As indicated by the NAO populations (cf. Table VII), s-orbitals dominate the central metal valence space. A little p_z- and even less d-occupation (from the totally symmetrical $d_{x^2-y^2}$ and d_{z^2} NAOs) complete the valence population for the linear species. Thus, natural population analysis indicates polar covalent bonding for the central metal with predominant s-character and some polarization by p- and d-orbitals toward the ligands. In valence bond terminology this may be interpreted as contributions from some sp- and sd-hybridization. In these less ionic MLi_2 and $M(BeH)_2$ species, the valence p-orbital participation exceeds the d-orbital contributions. This contrasts with all the other species (cf. Table VII) and contributes to the linear preferences for MLi_2, $Ca(BeH)_2$, and $Sr(BeH)_2$. Only $Ba(BeH)_2$ exhibits a nonlinear equilibrium geometry. As might be expected for the bent structure, the 5d-populations (with ca. 60% $5d_{yz}$ and ca. 40% totally symmetric 5d-NAO contributions) are larger than for the linear structure and exceed the contributions from 6p-NAOs. However, the 6s-occupation still dominates the valence populations and is larger than for the linear geometry.

Conclusions

The BaX_2 and SrX_2 compounds with a "first-row sweep" of substituents (X = Li to F) prefer distinctly bent structures ($BaLi_2$, $SrLi_2$, and $Sr(BeH)_2$ are the only exceptions). These results

(19) Schleyer, P. v. R. *Pure Appl. Chem.* **1987**, *59*, 1647.
(20) Westerhausen, M.; Schwarz, W. *Z. Anorg. Allg. Chem.*, in press.
(21) Vaartstra, B. A.; Huffman, J. C.; Steib, W. E.; Caulton, K. G. *Inorg. Chem.* **1991**, *30*, 121.
(22) Tilley, T. D.; Andersen, R. A.; Zalkin, A. *Inorg. Chem.* **1984**, *23*, 2271.
(23) Westerhausen, M.; Schwarz, W. *Z. Anorg. Allg. Chem.* **1991**, *604*, 127.
(24) Kaupp, M.; Schleyer, P. v. R., unpublished results.
(25) Lappert, M. F.; Power, P. R.; Sanger, A. R.; Srivastava, R. C. *Metal and Metalloid Amides*; Wiley: 1980; p 466ff.
(26) den Haan, K. H.; de Boer, J. L.; Teuben, J. H.; Spek, A. L.; Kojic-Prodic, B.; Hays, G. R.; Huis, R. *Organometallics* **1986**, *5*, 1726.

demonstrate that the bent structures of some monomeric barium and strontium dihalides[3-5] are not exceptional. But the first-row substituent effects are not monotonous. The smallest XMX angle is predicted for $Ba(CH_3)_2$ (115.9°), a value even lower than that for BaF_2 (125.6°). $P_\pi \rightarrow d_\pi$ donor interactions for X = NH_2, OH, F tend to widen the XMX angles. These π-contributions also may lead to significant rotational barriers in heavy alkaline earth amides. This conclusion receives some support from experimentally observed conformational preferences in some amide X-ray structures.[20-22] The availability of metal d-orbitals to act both as σ- and as π-acceptors offers an explanation for the similarities of the heavy alkaline earth structural organometallic chemistry to that of early transition-metal and f-block elements. Covalent contributions are important for the molecular geometries even though they constitute only a minor fraction of the total bonding energy in most of the highly ionic alkaline earth compounds (estimates of the heterolytic bonding energies of the dihalides based purely on coulombic considerations usually approximate the experiment closely[27]). A similar conclusion was reached regarding the significance of $p_\pi \rightarrow d_\pi$ bonding contributions for the more covalent early transition-metal amides, based on thermochemical and structural data.[25] Further computational studies will help assess the importance of the covalent d-orbital contributions, e.g., in the bioinorganic chemistry of Ca, Sr, and Ba.

(27) Hildenbrand, D. L. *J. Electrochem. Soc.* **1979**, *126*, 1396.

Acknowledgment. This work was supported by the Deutsche Forschungsgemeinschaft, the Fonds der Chemischen Industrie, the Stiftung Volkswagenwerk, and Convex Computer Corporation. M.K. acknowledges a Kekulé grant by the Fonds der Chemischen Industrie. We thank Prof. H. Stoll (Stuttgart) for stimulating discussions, Dr. M. Westerhausen (Stuttgart) for experimental results prior to publication, and Prof. A. Streitwieser, Jr. (Berkeley) for initiating our interest in the calcium fluoride problem.

Registry No. $CaLi_2$, 12013-43-3; $Ca(BeH)_2$, 137668-54-3; $Ca(BH_2)_2$, 137668-51-0; $Ca(CH_3)_2$, 19180-99-5; $Ca(NH_2)_2$, 23321-74-6; $Ca(OH)_2$, 1305-62-0; CaF_2, 7789-75-5; $SrLi_2$, 137718-23-1; $Sr(BeH)_2$, 137668-55-4; $BaLi_2$, 137718-22-0; $Ba(OH)_2$, 17194-00-2; BaF_2, 7787-32-8; $Ba(NH_2)_2$, 20253-29-6; $Ba(CH_3)_2$, 84348-36-7; $Ba(BeH)_2$, 137668-56-5; $Ba(BA_2)_2$, 137668-52-1; $Sr(OH)_2$, 18480-07-4; $Sr(BH_2)_2$, 137668-53-2; $Sr(CH_3)_2$, 108899-22-5; SrF_2, 7783-48-4; $Sr(NH_2)_2$, 23731-24-0.

Finite T_d Symmetry Models for Diamond: From Adamantane to Superadamantane ($C_{35}H_{36}$)

Mingzuo Shen,[†] Henry F. Schaefer III,*[,†] Congxing Liang,[†] Jenn-Huei Lii,[‡] Norman L. Allinger,[‡] and Paul von Ragué Schleyer[‡,§]

Contribution from the Department of Chemistry, University of Georgia, Athens, Georgia 30602.
Received May 6, 1991

Abstract: Seven clusters based on the diamond lattice, ranging in size from cyclohexane (C_6H_{12}, D_{3d}) to the "adamantane-of-adamantanes" (or superadamantane-5, $C_{35}H_{36}$, T_d), have been computed by molecular mechanics (MM2 and MM3), semiempirical self-consistent-field (SCF) (MINDO/3, MNDO, AM1, and PM3) methods, and ab initio SCF (with the minimal STO-3G, DZ, and DZP basis sets) theory. Molecular geometries are fully optimized under appropriate symmetry constraints in the MM2, MM3, and ab initio SCF methods, and by using Cartesian coordinates using semiempirical methods. Particular attention has been paid to the carbon–carbon bond lengths, total energies, and heats of formation. The largest cluster studied here is still far from the infinite diamond lattice. Comparisons among the computational methods reveal the merits and shortcomings of each.

Introduction

Owing to its composition, crystal structure, and mechanical, thermal, and electromagnetic properties, the diamond is unique. Its exceptional and favorable mechanical, thermal, and electromagnetic properties lead to wide-ranging industrial and engineering applications. Diamond research, particularly that involving thin films, continues to reveal new and important uses.[1-6]

Many physical properties of crystalline diamond are well established.[3,7,9] Each carbon atom in the diamond crystal is coordinated to four other carbons, with a carbon–carbon bond length of 1.5445 Å (X-ray).[8] The lattice is comprised of six-membered rings in chair conformations.[9]

Theoretical studies of diamond naturally fall into two broad categories: The first treats the diamond as an infinite lattice, while the second employs the finite cluster approximation. Sauer[10] analyzes these models from a chemist's point of view, emphasizing the crystal orbital and related solid-state physics approaches. Crystal orbital theory has been reviewed comprehensively by Pisani, Dovesi, and Roetti[11] recently.

The finite molecular approximation to infinite structures is frequently adopted by chemists.[10] In particular, fragments of the diamond lattice may be saturated by hydrogen atoms. This approach may be used to investigate the convergence behavior of

[†] Center for Computational Quantum Chemistry, University of Georgia.
[‡] Department of Chemistry, University of Georgia.
[§] Universität Erlangen-Nürnberg.

(1) Champion, F. C. *Electronic Properties of Diamond*; Butterworth: London, 1963.
(2) Berman, R. *Physical Properties of Diamond*; Oxford University Press: Oxford, England, 1965.
(3) Fields, J. E., Ed. *The Properties of Diamond*; Academic Press: London, 1979. This book has chapters on research in theoretical and experimental solid-state physics, surface science, mechanics, artificial growth, geology, and industrial applications and a table of the properties of diamond.
(4) Guyer, R. L.; Koshland, D. E. Diamond: glittering prize for materials science. *Science* **1990**, *250*, 1640. Diamond (including diamond films) is featured in this news article as the molecule of the year 1990. The runners-up include the C_{60} buckminsterfullerene molecule.
(5) Whitesides, G. M. What will chemistry do in the next twenty years? *Angew. Chem., Int. Ed. Engl.* **1990**, *29*, 1209. In this review, "very large" chemistry, of which the diamond chemistry is representative, is featured as one of the limits to be explored in the future, along with "very small" and "very fast" chemistry.
(6) Anthony, T. R.; Banholzer, W. F.; Fleischer, J. F.; Wei, L.; Kuo, P. K.; Thomas, R. L.; Pryor, R. W. *Phys. Rev.* **1990**, *42B*, 1104.
(7) (a) Bimberg, D.; Blacknik, R.; Cardona, M.; Dean, P. J.; Grave, T.; Harbeke, G.; Hübner, K.; Kaufmann, U.; Kress, W.; Madlung, O.; von Münch, W.; Rössler, U.; Schneider, J.; Schulz, M.; Skolnick, M. S. Physics of Group IV Elements and III-V Compounds. In *Landolt-Börnstein Numerical Data and Functional Relationships in Science and Technology*; New Series; Hellewe, K.-H., Ed.; Group III, Crystal and Solid State Physics, Vol. 17, Semiconductors; Madlung, O., Schulz, M., Weiss, H., Eds.; Subvol. a; Springer-Verlag: New York, 1982; pp 36-42.

0002-7863/92/1514-497$03.00/0